Universal soft pneumatic robotic gripper with variable effective length

HAO Yufei, GONG Zheyuan, XIE Zhexin, GUAN Shaoya, YANG Xingbang, REN Ziyu, WANG Tianmiao, WEN Li*

School of Mechanical Engineering and Automation, Beihang University, Beijing, 100191
E-mail: liwen@buaa.edu.cn

Abstract: In this study, we built a four-fingered soft robotic gripper with tunable effective finger lengths. This robotic model is purely made of soft materials and allows two working modes that require very simple control: 1) deflate the soft fingers for bending to one direction therefore to open the gripper "claw" and 2) inflate the fingers with compressed air for bending to the reverse direction, therefore to grip objects reversibly. Systematic tests of the gripping performance of the soft robotic model were conducted for 5 effective finger lengths ranging from 30 mm to 100 mm. Under each effective length, we measured the pull-off force of 8 sphere-shaped objects with diameters from 20 to 90mm, and five typical geometric shaped objects including sphere, cubic and cylinder etc. We also measured the pull-off force of gripping objects with different stiffness. Notably, we found that each object with different size prefer a "sweet" effective finger length for generating maximum pull-off force. We show that tunable effective finger length for the soft robot can significantly improve the performance when gripping multiple objects. Current soft robotic prototype exhibits a simple-control, low-cost approach of grasping objects with different size, weight, and shape as well as material stiffness, and may open up new avenues for future industrial gripping.
Key Words: Soft robotics, pneumatic actuation, gripper

1 Introduction

Soft robotics is a new member of robotic family that has several promising features, such as lightweight, inexpensive, easily fabricated, simply to control etc.[1]-[3]. Recently, design, fabrication and actuation of soft robotics have attracted growing attentions of researchers from multiple fields such as chemistry [4][5], physics [6], biology [7][8]and mechanical engineering [9][10]. The soft robotics can be fabricated by several approaches including multi-material 3D printing [11]-[13], shape deposition manufacturing (SDM) [14], soft lithography [15]-[17], or integrate multiple manufacturing approaches to create composite materials [18]-[20]. Variable length tension cables driven [21]-[23], pneumatic or hydraulic for inflation of channels in a soft material [15][24], and electro-active polymers or shape memory alloy were usually used for the actuation of soft robotics [25][26]. While integrating multiple segments of soft actuators have made several applications possible, for example, wearable human rehabilitation device [27]-[29], bio-inspired robotic locomotion [15][30]-[33] and human-machine interaction[2].

Recall that, conventional rigid robotic grippers typically use two or more fingers that require visual feedback and force sensing at the fingertips and a central processor running algorisms and make decisions before gripper touches the object for achieve adaptive grasping. Therefore rigid multi-fingered gripper is a complex system to implement and hard to control. A universal gripper based on soft material actuation may have a variety of applications where different objects that need to be gripped reliably and in rapid succession [6][21]. Very recently, companies (for example, Soft Robotics Inc.) also have begun to produce commercially developed simple soft pneumatic elastomeric gripper which showed some capabilities of manipulate lightweight objects. However, no systematic characterization of gripping performance was conducted and many questions remain. What is maximum gripping weight does a soft pneumatic gripper can perform? Does a single soft elastomeric gripper allow objects with multiple size and shapes to be gripped? Are there any fundamental mechanisms for explaining the gripping performance? To scientifically address the above questions, we need to implement experimental device that allows forces on objects with different size, shape and material stiffness to be measured. To our knowledge, no systematic force measurements were conducted for any soft pneumatic gripper.

In this paper, we focused on a simple form of a soft gripper, a four-fingered pneumatic actuated elastomeric robot that approximate the biological finger with infinite degrees of freedom. This robot only requires simple control for pneumatically actuation: deflating the soft actuators to open the gripper claw to approach the objects, then inflate the soft actuators to contact with the surface of the objects to be gripped. Then we used a selectively-placed nylon tendon that acts to mechanically change the finger area of inflation and deflation (we term the length of this area as "effective length of the robotic finger"). We quantified the gripper's displacement of deformation and pull-off force while gripping objects with different shape and size under a number of effective finger lengths and pneumatic air pressures. Based on the experimental results, we formulated several hypothesis of the gripping mechanisms.

2 Materials and Methods

2.1 Design and Fabrication of the Soft robotic gripper

From mechanical design aspect, the single soft finger element was mainly consist of three components (Fig. 1(a)): 1) the soft elastomeric finger, 2) the fixator which was used to fasten and connect the soft finger to the support, and was 3D printed with poly lactic acid (PLA) material, 3) the tube joint that allowed the compressed air to inflate/deflate the soft finger. Four pneumatically actuated soft elastomeric finger were integrated on a 3D printed rigid base support (Fig. 1(b)). The lower part of the tube joint was inserted into the air inlet (Fig. 2(e)) of the soft finger and the other part was connected with the air tube (Fig. 1(a)). The tube joint and the fixator were fastened with bolts in order to seal the air channel and to avoid air leakage.
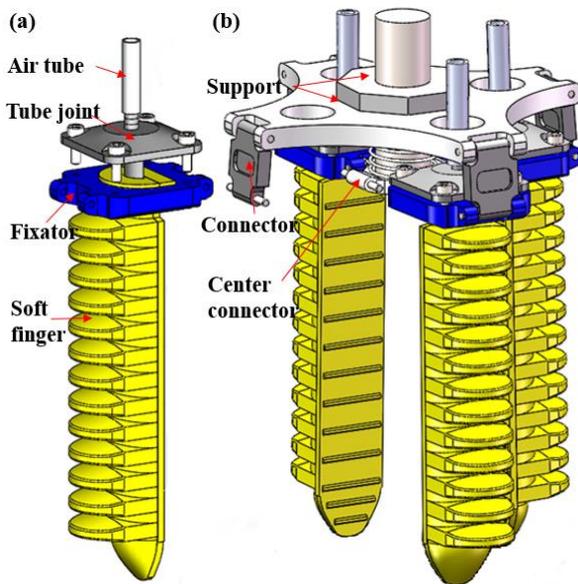

Figure 1. The design of the soft robotic gripper. (a) The soft finger element, composed of four components: the air tube, the tube joint, the fixator and the soft finger. (b) The 3D structure of the soft robotic gripper. The soft finger elements were connected to the support using connectors

The soft finger was fabricated by using purely soft silicone elastomeric material (dragon skin 30, smooth-on Inc., USA). The rigid molds were designed in Solidworks (SolidWorks Corp., Waltham, MA, USA) and were fabricated using PLA material by 3D printing; its simplicity allowed us to iteratively fabricate quickly. The multi-step molding process of a single soft actuator is shown in Fig. 2. Note that the fabrication process was inspired from the fabrication of Harvard pneumatic-net soft robotic actuators[17] The upper molds A and B (see Fig. 2(a)) were fabricate to form the extensible top layer that contains topographical features. The bottom mold was used for the inextensible bottom layer part of the soft finger. Firstly, the uncured silicone rubber material was poured into the molds. The molds and uncured materials were then put in a vacuum oven for 30min for degassing, therefore to remove the air bubbles, and were then heated to a temperature of 60℃ for 2h in order to cure the material. Finally, the parts were demold and then bonded together by applying a thin layer of silicone rubber on the bonding surface. By inflation or deflation, the soft actuator that contains topographical feature would expand or shrink, which further resulted in bending in either convex or concave states (see Fig. 3(a) for notation).
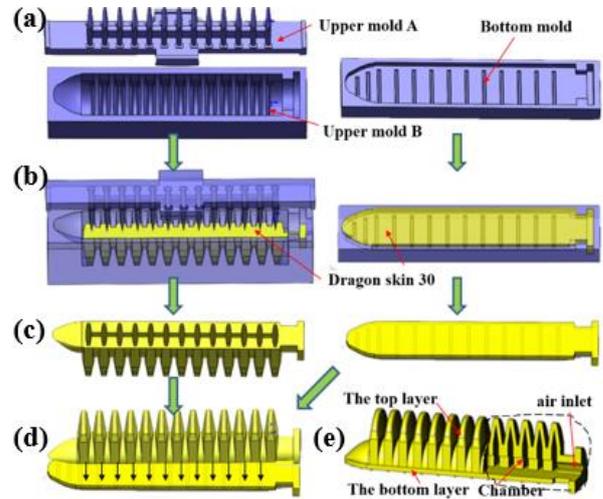

Figure 2. Schematic of the single soft finger fabrication process. (a) Both the upper molds A, B and the bottom mold were fabricated by 3D printing. (b) Silicone rubber (Dragon skin 30) was poured into the upper mold B. Then the upper mold A was forced into the upper mold B that was filled with uncured material. (c) Both top layer and bottom layer of soft actuator were removed from the 3D printed rigid molds after cured. (d) The top layer with topographical features and the bottom layer were bond together; the black arrows indicate the bonding direction. (e) The overview of the soft finger with a cross section view which schematically illustrate the topographical features, the inner chamber and the air inlet.

To characterize the kinematics of the soft finger, we inflated the soft finger to a certain pressure and captured the kinetic data of the finger under different pressures (from -40 kPa to 50 kPa as show in Fig. 3(a)). We also digitized the profile curves of the finger during motion by using a Matlab program (Fig. 3(b) and (c)). We found that the finger-tip amplitude of the finger ranges from -80mm to 65mm in the X direction and 0 to 110mm in the Y direction.

Inspired by the bi-directional bending feature of the soft finger, we proposed a novel approach for gripping objects: deflating the soft fingers to curl the fingers outwards, i.e., open the gripper claw (see Fig. 3(d)) and approach the objects. Then the chamber will be inflated with compressed air and the fingers will curl inwards to contact with the surface of the objects to be gripped (Fig. 3(e)). Further increasing the inflating air pressure would allow the objects to be conformed by the gripper. We used a One-Touch Fitting (KQ2UD04, SMC, Japan) to converge the air inlet tube to four tubes that connect each of the four soft finger, therefore all fingers could be inflated simultaneously. The air tube is connected to an electro-pneumatic proportional pressure valve (ITV0030, SMC, Japan) which was used to control the output air pressure by changing the input voltage. In addition, we used a selectively-placed nylon tendon that acted to mechanically change the finger area of inflation and deflation. We term the length of this area as "effective length of the robotic finger" (see Fig. 4 for notation).

2.2 Experimental setup for characterizing the gripping force

In order to evaluate the gripping performance of the prototype, we set up an experimental platform to test the pull-off force while maintaining the key feature of a true gripping process. To that end, we kept the object fixed and pulled the gripper vertically up at a constant speed (see Fig. 4(a)). The gripped object was connected with a six-axis force transducer (Mini 40 F/T sensor, ATI) fixed to a mounting base. The bottom side of the force transducer was concretely mounted to an optical table. The connecting rod can be moved vertically up through the slide and pull the soft gripper up and away from the gripped object. During each experimental trial, we first biased the weight of the object in force acquisition Labview program. Then the soft fingers will be inflated to a defined pressure and conformed the test object. Afterwards the gripper was moved upwards at a constant speed of 18 mm/s until the gripper was completely detached from the object which took about 5s. During this gripping process, the force data in Z axis was recorded simultaneously at a sampling rate of 500Hz. Here in this study, the pull-off force was defined as the maximum force generated during the whole gripping process. Instantaneous force data was filtered by using a low-pass filter (15Hz). The average value of 5 maximum peak forces was finally used for calculating the pull-off force of each measurement.

In order to test the relationship between the pull-off force and the size of the gripped object under different tunable effective length of the finger, we 3D printed 8 sphere-shaped objects with different diameters ranging from 20 mm to 90 mm with interval of 10mm. While characterizing the force performance, different effective finger lengths were set before the test for each gripped object (30, 50, 65, 80, and 100mm). In addition, three air pressures were chosen to inflate the soft gripper (30, 50, and 70 kPa). For this experiment, over 120 experimental cases were conducted totally, while 5 replicate trials were performed for each case to obtain the mean data. To sum up, over 600 trials were carried out. We also performed pull-off force experiments to investigate the effect of the shape of gripped objects. Six objects of different shapes with equal circumscribed spheres (sphere, cylinder, cuboid, cube, eight-angular prism and square pyramid) were 3D printed. Then we tested the pull-off force for each of above objects under a fixed effective finger length (100 mm) and air pressure (50 kPa). Finally, to validate the universality of the soft gripper, we used it to grip some common items with different sizes, shapes and stiffness in our daily life.
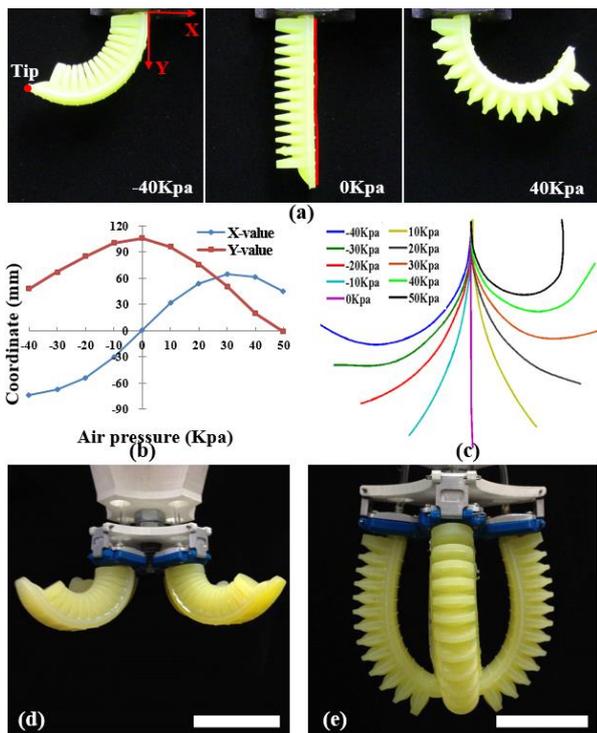

Figure 3. Kinematics of single soft finger and the soft gripper. (a) Images of the single soft finger deformations under air pressure of deflation (-40 kPa), depressurization (0 kPa) and inflation (40 kPa). Both "finger-tip" and profile of the bottom layer of the actuator are marked in red. (b) The tip displacement of the soft finger vs. air pressure. (c) Profiles of the actuator's bottom layer under different positive pressure for inflation and negative pressure for deflation. (d) The four-fingered soft gripper under deflation state with a tip-tip distance of 150mm. The scale bar is 50 mm. (e) the soft robotic gripper under pressurized state. The scale bar is 50 mm.
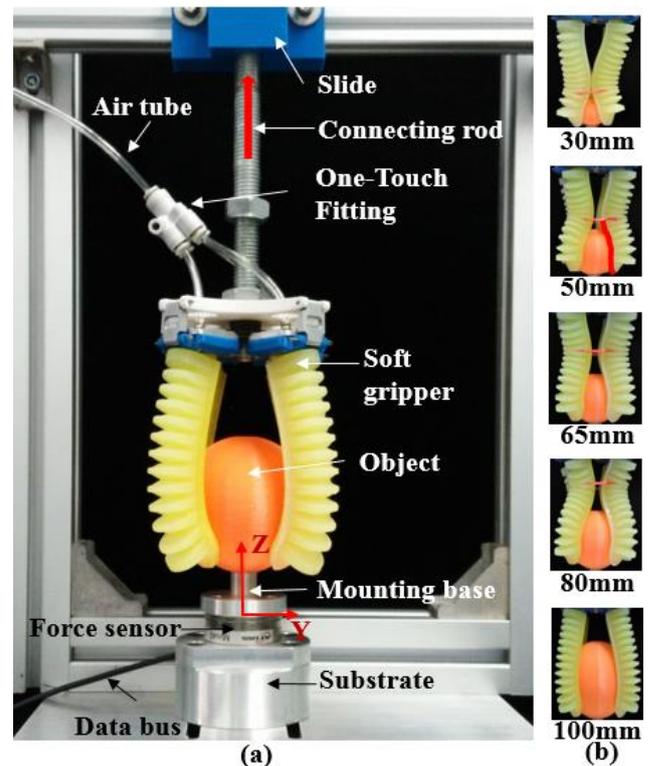

Figure 4. Apparatus for measuring force of the soft gripper under different effective lengths. (a) Schematic illustration of the force measurement platform. The object was fixed to the six-axis force transducer via a mounting base. During each experimental trial, compressed air was inflated into the soft finger thus to allow it to conform the object. When the soft gripper was then pulled vertically upwards along the slide at speed of 18 mm/s, the force data was recorded simultaneously. (b) Images of the soft robotic gripper under five selected effective finger lengths while gripping. We used an inelastic nylon tendon to bind the fingers therefore to change the length of the finger that inflate. Effective length of the soft finger is marked by a red solid line in panel b (when length is 50 mm).

3 Results

3.1 Effect of finger lengths and pressures on gripped objects of different sizes

Fig. 5 shows the pull-off force results as function of the size of the objects, the effective length and the air pressure. It can be observed that, except the case of 100 mm-length, the pull-off forces under the other 4 tested effective finger lengths uniquely exhibited profiles shape of "reversed parabola", which gradually increased to a maximum peak and then decreased as the sphere diameter increased. Therefore, there exists an optimal length with the maximum pull-off force for a specific gripped size. It was quite noteworthy that, the peak values of the five curves appeared at different diameters, soft gripper with longer/shorter effective length preferred larger/smaller diameter of sphere. It was also quite interesting that, under the same air pressure, the diameters of sphere did not significantly affect the peak values of pull-off force. From Fig. 5 (a) to (c), increasing air pressure from 30 kPa to 70 kPa, the averaged pull-off forces increased around 3 times.
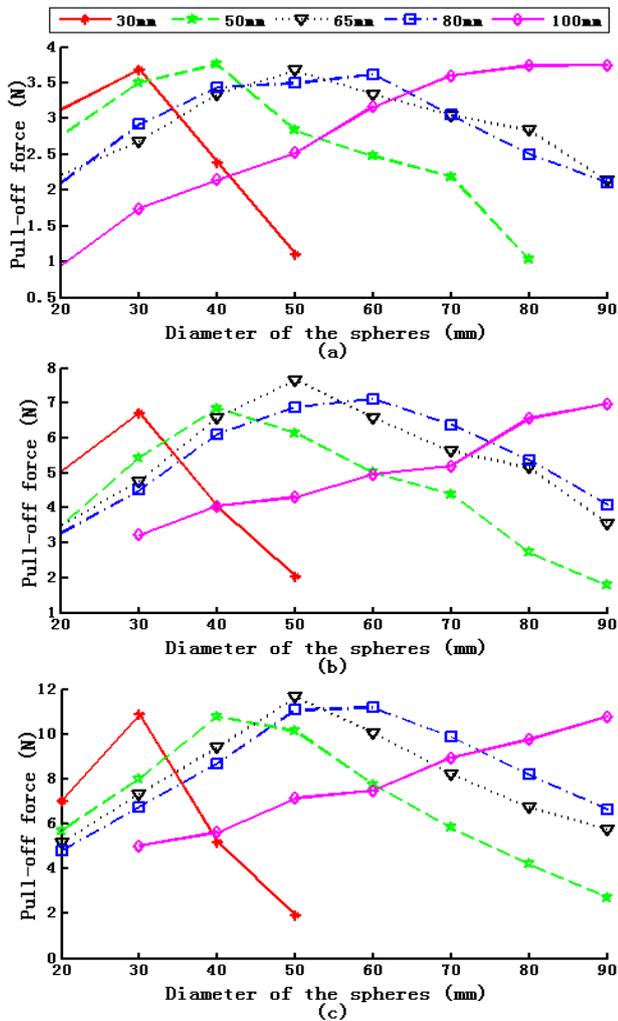

Figure 5. Pull-off force versus the diameter of sphere as function of effective finger length under pneumatic actuated pressures of (a) 30 kPa, (b) 50 kPa and (c) 70 kPa. The pull-off forces are averaged from *N*=5 trials for each measurements. The calculated standard errors of the data range from 0.005 N to 0.185 N, which are relatively small compared with the mean force value, therefore they were not shown in this graph.

3.2 Gripping objects with different shapes

Fig. 6 shows the pull-off force as function of different shapes of objects. It is quite obvious that the shape of the objects have a significant impact on the pull-off force. We divided the shapes of objects into three groups based on the force values. Group-I (Fig. 6C: the cuboid) generated the minimal pull-off force, group-II (Fig. 6A and B: the sphere and the cylinder) resulted in mediate pull-off force, while group-III (Fig. 6D, E and F: the cube, the eight-angular prism and the square pyramid) resulted in the maximum pull-off force. In group I (when gripping the cuboid), the gripper conformed and contacted with cuboid on its vertical sides, the pull-off force was significantly smaller than the pull-off force of all other gripped objects. This may possibly due to the fact that friction force tangential to the surface plays dominate role in the pull-off force. In contrast, significantly larger pull-off forces were generated in group-III. In this case, the soft gripper conformed and enclosed the objects (see Fig. 6D-E) by extending the fingers below the bottom of the objects. This may due to a geometrical interlocking effect which takes over and dominates the pull-off force, whereas the friction force played a minor role. While gripping objects in group II (Fig. 6A and B), the soft fingers deformed along the objects' surface and generated intermediate pull-off force.
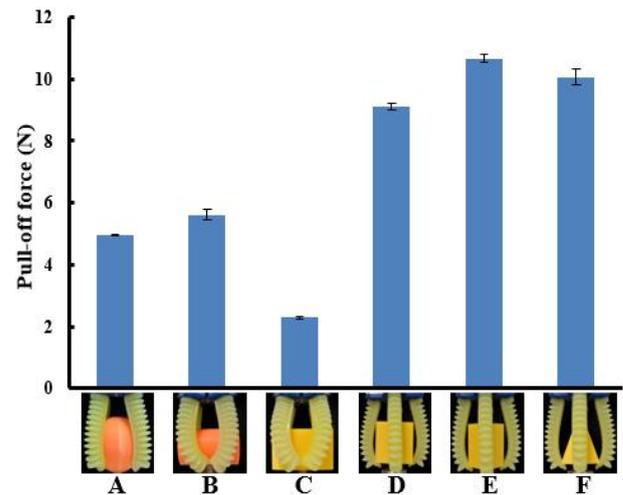

Figure 6. Pull-off force of the soft gripper as function of different shapes of objects at 50 kPa, and under effective length of 100 mm. A: sphere, B: cylinder, C: cuboid, D: cube, E: eight-angular prism, F: square pyramid.

3.3 Multiple objects

By simply controlling the air pressure and the effective finger length, the soft gripper demonstrated ability of gripping a wide range of objects, including those tested objects in Fig. 5 and 6 but also many other items with different size, shape and stiffness. For example, the gripper can pick up a rectangular shaped box with the dimension of 16 cm in length and 11 cm in width (Fig. 7(a)); It can grip complex shaped objects such as wood carving hand (Fig. 7(b)), or even a cactus with spines (Fig. 7(c)); It can grip a tiny screw with diameter of 2mm (Fig. 7(d)) or a pen (Fig. 7(e)), or a chain of keys (Fig. 7(f); It can also grasp a bag of milk (Fig. 7(i)), a compact disc (Fig. 7(g)) and a raw chicken

egg (Fig. 7(h)). It should be noted that, gripping soft, fragile and flatten objects is difficult to achieve by using the traditional robotic grippers and the universal jamming gripper [6] [34], however, can be easily achieved by current soft pneumatic gripper.
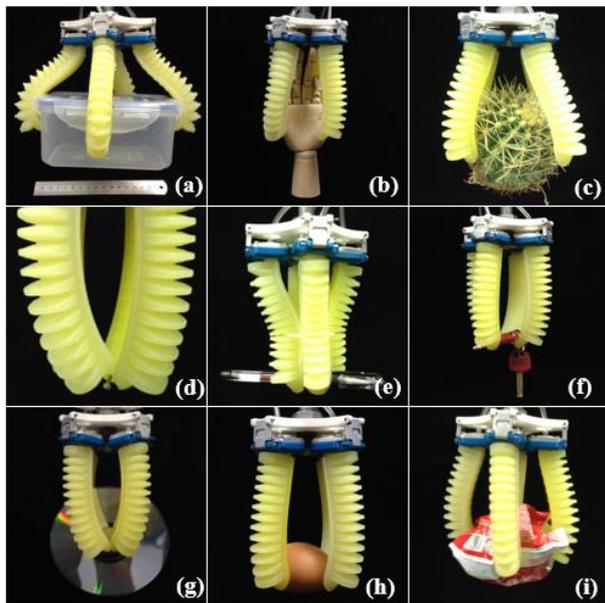

Figure 7.Results of universality of the soft gripper. The soft gripper can be applied to grasp objects with different shape, size and stiffness. (a) rectangular-shaped box with a dimension of 16cm in length and 11cm in width, (b) a wooden model for human hand, (c) cactus, (d) a screw, (e) a pen, (f) a chain of keys, (g) a compact disk, (h) a raw chicken egg and (i) a bag of milk.

4 Discussion And Conclusion

Our results demonstrated how a pneumatic actuated elastomeric gripper associated with an inflation/deflation transition enables it to grip a wide range of different objects reliably. The kinematics of the current soft gripper showed a possible object size range up to 160 mm, which is similar to that of the human hand [34]. We tested the pull-off force of the gripper as function of object size, shape and material stiffness under a range of effective finger lengths. A maximum pull-force of 13.5N was observed according to all experimental trials in this study. With addition of tunable effective finger lengths, the soft gripper can easily grip objects larger than itself (Fig. 7(a)), a plastic bag filled with milk (Fig. 7 (i)) and a compact disc (Fig. 7(g)) etc. These items, to our knowledge, are difficult to manipulate by using some famous universal robotic gripper prototypes, such as the jamming gripper [6].

Systematic tests of the gripping performance of the soft robotic model were conducted for 5 effective finger lengths ranging from 30 mm to 100 mm. Under each effective length, we measured the pull-off force of gripped objects with different sizes and pneumatic pressures. Under each pressure, when the diameter of the sphere gradually increased, the pull-off force uniquely exhibited profiles shape of "reversed parabola". Notably, we found that each object with different size prefer a "sweet" effective finger length for generating maximum pull-off force. We consider the soft robotic gripper with effective finger length has potential applications in industrial manipulation. It can be imagine that, one can easily grip objects with different size by settling the soft robotic gripper to the "sweet" effective finger length, instead of changing the whole manipulator.

We hypothesize that the gripper achieves its pull-off force through effects of friction and geometrical interlocking. Evidence for this hypothesis could be reflected by the experimental data. For example, when gripping objects with vertical sides of cuboid, the pull-off force was significantly smaller than the pull-off force of all other gripped objects (see Fig. 6C for notation), as the friction force tangential to the surface played dominate role in the pull-off force. In contrast, the soft gripper conformed and enclosed the object such as sphere and cubic-shaped objects (see Fig. 6A, D-E), a geometrical interlocking effect would take over and dominate the pull-off force, whereas the friction force played a minor role. As a result, when the robot grips cubic-shaped objects, the maximum pull-off force was around 2 times larger than that of the sphere-shaped object.

For the ongoing work, we are investigating the geometrical effect of the soft robotics and material stiffness using both Finite Element Analysis (FEA) simulations and experiments. We are also quantitatively elevating the gripping speed and precision of pick-place of the soft gripper as well.

References

[1] H. Lipson, "Challenges and Opportunities for Design, Simulation, and Fabrication of Soft Robots," *Soft Robotics*, 2013.

[2] D. Rus, and M. T. Tolley, "Design, fabrication and control of soft robots," *Nature,* vol. 521, pp. 467-75, 2015.

[3] S. Kim, C. Laschi, and B. Trimmer, "Soft robotics: a bioinspired evolution in robotics," *Trends in Biotechnology,* vol. 31, no. 5, pp. 23-30, May, 2013.

[4] F. Ilievski, A. D. Mazzeo, R. E. Shepherd, X. Chen, and G. M. Whitesides, "Soft Robotics for Chemists," *Angewandte Chemie-International Edition,* vol. 50, no. 8, pp. 1890-1895, 2011.

[5] R. F. Shepherd, A. A. Stokes, J. Freake, J. Barber, P. W. Snyder, A. D. Mazzeo, L. Cademartiri, S. A. Morin, and G. M. Whitesides, "Using Explosions to Power a Soft Robot," *Angewandte Chemie-International Edition,* vol. 52, no. 10, pp. 2892-2896, 2013.

[6] E. Brown, N. Rodenberg, J. Amend, A. Mozeika, E. Steltz, M. R. Zakin, H. Lipson, and H. M. Jaeger, "Universal robotic gripper based on the jamming of granular material," *Proceedings of the National Academy of Sciences of the United States of America,* vol. 107, no. 44, pp. 18809-18814, Nov 2, 2010.

[7] L. J. H. Jr., CombesStacey, NawrothJanna, HaleMelina, LauderGeorge, SwartzSharon, QuinnRoger, and ChielHillel, "How Does Soft Robotics Drive Research in Animal Locomotion?," *Soft Robotics*, 2014.

[8] Ren, Z., Yang, X., Wang, T., and Wen, L.," Hydrodynamics of a robotic fish tail: effects of the caudal peduncle, fin ray motions and the flow speed", *Bioinspiration & Biomimetics*, vol.11,no.1, 2016.

[9] R. Deimel, and O. Brock, "A novel type of compliant, underactuated robotic hand for dexterous grasping," *Robotics: Science and Systems, Berkeley, CA*, pp. 1687-1692, 2014.

[10] P. Polygerinos, Z. Wang, J. T. B. Overvelde, K. C. Galloway, R. J. Wood, K. Bertoldi, and C. J. Walsh, "Modeling of Soft Fiber-Reinforced Bending Actuators," *IEEE Transactions on Robotics,* vol. 31, no. 3, pp. 778-789, Jun, 2015.

[11] N. W. Bartlett, M. T. Tolley, J. T. B. Overvelde, J. C. Weaver, B. Mosadegh, K. Bertoldi, G. M. Whitesides, and R. J. Wood, "A 3D-printed, functionally graded soft robot powered by combustion," *Science,* vol. 349, no. 6244, pp. 161-165, Jul 10, 2015.

[12] Wen, L., Weaver, J. C., Thornycroft, P. J., and Lauder, G. V. , "Hydrodynamic function of biomimetic shark skin: effect of denticle pattern and spacing", *Bioinspiration & Biomimetics*, vol.10,no.6,2015.

[13] Wen, L., Weaver, J. C., and Lauder, G. V., "Biomimetic shark skin: design, fabrication and hydrodynamic function", *Journal of Experimental Biology,* vol.217,no.10, pp. 1656-1666,2014.

[14] S. A. Suresh, D. L. Christensen, E. W. Hawkes, and M. Cutkosky, "Surface and Shape Deposition Manufacturing for the Fabrication of a Curved Surface Gripper," *Journal of Mechanisms and Robotics-Transactions of the Asme,* vol. 7, no. 2, May, 2015.

[15] R. F. Shepherd, F. Ilievski, W. Choi, S. A. Morin, A. A. Stokes, A. D. Mazzeo, X. Chen, M. Wang, and G. M. Whitesides, "Multigait soft robot," *Proceedings of the National Academy of Sciences of the United States of America,* vol. 108, no. 51, pp. 20400-20403, Dec 20, 2011.

[16] S. A. Morin, R. F. Shepherd, S. W. Kwok, A. A. Stokes, A. Nemiroski, and G. M. Whitesides, "Camouflage and Display for Soft Machines," *Science,* vol. 337, no. 6096, pp. 828-832, Aug 17, 2012.

[17] R. F. Shepherd, A. A. Stokes, R. M. D. Nunes, and G. M. Whitesides, "Soft Machines That are Resistant to Puncture and That Self Seal," *Advanced Materials,* vol. 25, no. 46, pp. 6709-6713, Dec, 2013.

[18] K. J. Cho, J. S. Koh, S. Kim, W. S. Chu, Y. Hong, and S. H. Ahn, "Review of manufacturing processes for soft biomimetic robots," *International Journal of Precision Engineering and Manufacturing,* vol. 10, no. 3, pp. 171-181, Jul, 2009.

[19] A. A. Stokes, R. F. Shepherd, S. A. Morin, F. Ilievski, and G. M. Whitesides, "A Hybrid Combining Hard and Soft Robots," *Soft Robotics,* vol. 1, no. 1, pp. 70-74, 2014.

[20] F. Connolly, P. Polygerinos, C. J. Walsh, and K. Bertoldi, "Mechanical Programming of Soft Actuators by Varying Fiber Angle," *Soft Robotics,* vol. 2, pp. 26-32, 2015.

[21] L. U. Odhner, L. P. Jentoft, M. R. Claffee, N. Corson, Y. Tenzer, R. R. Ma, M. Buehler, R. Kohout, R. D. Howe, and A. M. Dollar, "A compliant, underactuated hand for robust manipulation," *International Journal of Robotics Research,* vol. 33, no. 5, pp. 736-752, Apr, 2014.

[22] C. H. Yeow, A. T. Baisch, S. G. Talbot, and C. J. Walsh, "Cable-Driven Finger Exercise Device With Extension Return Springs for Recreating Standard Therapy Exercises," *Journal of Medical Devices-Transactions of the Asme,* vol. 8, no. 1, Mar, 2014.

[23] H. S. Stuart, W. Shiquan, B. Gardineer, D. L. Christensen, D. M. Aukes, and M. Cutkosky, "A compliant underactuated hand with suction flow for underwater mobile manipulation." pp. 6691-6697.

[24] B. Mosadegh, P. Polygerinos, C. Keplinger, S. Wennstedt, R. F. Shepherd, U. Gupta, J. Shim, K. Bertoldi, C. J. Walsh, and G. M. Whitesides, "Pneumatic Networks for Soft Robotics that Actuate Rapidly," *Advanced Functional Materials,* vol. 24, no. 15, pp. 2163-2170, Apr, 2014.

[25] Q. Shen, T. Wang, J. Liang, and L. Wen, "Hydrodynamic performance of a biomimetic robotic swimmer actuated by02ionic polymer–metal composite," *Smart Materials &*

Structures, vol. 22, no. 7, pp. 2896-2912, 2013.

[26] S. Seok, C. D. Onal, K. J. Cho, R. J. Wood, D. Rus, and S. Kim, "Meshworm: A Peristaltic Soft Robot With Antagonistic Nickel Titanium Coil Actuators," *Ieee-Asme Transactions on Mechatronics,* vol. 18, no. 5, pp. 1485-1497, Oct, 2013.

[27] Y. L. Park, B. R. Chen, N. O. Perez-Arancibia, D. Young, L. Stirling, R. J. Wood, E. C. Goldfield, and R. Nagpal, "Design and control of a bio-inspired soft wearable robotic device for ankle-foot rehabilitation," *Bioinspiration & Biomimetics,* vol. 9, no. 1, Mar, 2014.

[28] T. Noritsugu, M. Takaiwa, and D. Sasaki, "Power Assist Wear Driven with Pneumatic Rubber Artificial Muscles." pp. 539-544.

[29] D. Ye, I. Galiana, A. Asbeck, B. Quinlivan, S. M. M. De Rossi, and C. Walsh, "Multi-joint actuation platform for lower extremity soft exosuits." pp. 1327-1334.

[30] K. Suzumori, S. Endo, T. Kanda, N. Kato, and H. Suzuki, "A Bending Pneumatic Rubber Actuator Realizing Soft-bodied Manta Swimming Robot." pp. 4975-4980.

[31] M. Calisti, M. Giorelli, G. Levy, B. Mazzolai, B. Hochner, C. Laschi, and P. Dario, "An octopus-bioinspired solution to movement and manipulation for soft robots," *Bioinspiration & Biomimetics,* vol. 6, no. 3, Sep, 2011.

[32] C. Laschi, M. Cianchetti, B. Mazzolai, L. Margheri, M. Follador, and P. Dario, "Soft Robot Arm Inspired by the Octopus," *Advanced Robotics,* vol. 26, no. 7, pp. 709-727, 2012.

[33] C. D. Onal, and D. Rus, "Autonomous undulatory serpentine locomotion utilizing body dynamics of a fluidic soft robot," *Bioinspiration & Biomimetics,* vol. 8, no. 2, Jun, 2013.

[34] J. R. Amend, E. Brown, N. Rodenberg, H. M. Jaeger, and H. Lipson, "A Positive Pressure Universal Gripper Based on the Jamming of Granular Material," *IEEE Transactions on Robotics,* vol. 28, no. 2, pp. 341-350, Apr, 2012.